half of a complete discharge. This makes recharging difficult and reduces cycle life.

Conclusion

The Cd_2SnO_4 electrode prepared by isostatic pressing of $2CdO:1SnO_2$ powder mixture and consequent firing yields a porous body that proved to be an interesting electrode material for secondary battery applications. The relatively high conductivity of this compound eliminates some elaborate processes of conventional electrode fabrications. Chemical stability of Cd_2SnO_4 in basic media was established, which means a longer shelf-life. A constructed cell using Cd_2SnO_4 as negative electrode with 1.48V (o.c.) was proved to be stable up to 4 months time. Cyclic voltammetry experiments showed that the number of charge-discharge cycles was quite high before the coulombic efficiency drop. The present work revealed some novel features of Cd_2SnO_4 as the negative electrode in rechargeable battery systems. Deeper understanding of these interesting features and improvement of the performance calls for further investigations.

Manuscript submitted Sept. 8, 1986; revised manuscript received Dec. 12, 1986.

The Materials and Energy Research Centre, Tehran, assisted in meeting the publication costs of this article.

REFERENCES

1. L. C. Burton, T. Hench, G. Storti, and G. Haack, *This Journal*, **123**, 1741 (1976).
2. G. Haack, *Appl. Phys. Lett.*, **30**, 380 (1977).
3. K. J. D. Mackenzie, W. A. Gerrard, and F. Golestani-Fard, *J. Mater. Sci. Lett.*, **14**, 2509 (1976).
4. F. Golestani-Fard, T. Hashemi, K. J. D. Mackenzie, and C. A. Hogarth, *J. Mater. Sci.*, **18**, 3679 (1983).
5. R. P. Howson, M. I. Ridge, and C. A. Bishop, *Thin Solid Films*, **80**, 137 (1981).
6. N. Miyata, K. Miyake, K. Koga, and T. Fukushima, *This Journal*, **127**, 918 (1980).
7. D. Hall, *ibid.*, **124**, 804 (1977).
8. D. Hall, *ibid.*, **127**, 308 (1980).
9. T. Hashemi and F. Golestani-Fard, in "Proceedings of the 6th International Congress on Hi-Tec Ceramics," Milan, Italy, 1986, In press.
10. A. Kitani, M. Kaya, Y. Hiromoto, and K. Sasaki, *Denki Kagaku*, **53**, 592 (1985).

The Lead Anode in Alkaline Solutions

II. The Mechanism of PbO Film Formation

V. I. Birss* and M. T. Shevalier**

Chemistry Department, University of Calgary, Calgary, Alberta T2N 1N4, Canada

ABSTRACT

The mechanism of the initial stages of PbO formation has been investigated at a Pb anode in 1*M* NaOH solutions, with the use of cyclic voltammetry, transient and steady-state potential step methods, and modulated surface reflectance spectroscopy (MSRS). It has been found that, following the deposition and dissolution of $Pb(OH)_2$ at less positive potentials, PbO deposition initiates according to an instantaneous three-dimensional nucleation and growth mechanism under diffusion control. This is supported by the good match of the experimentally obtained i–t response with the theoretically predicted one, by the observed changes in surface reflectivity with time and the marked effects of electrode rotation on the observed currents. Some dissolution of PbO also occurs in these early stages of oxidation, forming the $HPbO_2^-$ species, consistent with the observed Tafel slope and the excess of the anodic to cathodic charge in cyclic voltammetry. At still higher potentials or longer times, very thick porous PbO films can be formed, consistent with film initiation by a nucleation and growth mechanism.

The remarkably high corrosion resistance of Pb in most neutral and acidic conditions has resulted in its use as a construction and containment material for many corrosive chemicals and in corrosive environments (1, 2). It has also led to the very successful combination of Pb and sulfuric acid in Pb/acid batteries (3). However, in alkaline solutions, it has been predicted (4) that Pb would be susceptible to corrosion, leading to the formation of soluble forms of lead and of various Pb oxides of uncertain stability. Therefore, our investigation has focused on understanding the electrochemical behavior of Pb and the properties of Pb oxides in alkaline solutions, commencing with a study of pH 14 solutions.

In a previous paper (5), it was shown that the first step in Pb oxidation in these solutions involves the formation and dissolution of a $Pb(OH)_2$ film, and the mechanism of these reactions was elucidated and described in detail. Using cyclic voltammetry (CV), as well as steady-state and transient potentiostatic methods, the following principal reactions ([1], [2], and [3]) were found to occur in the potential range of about 150-300 mV *vs.* RHE

$$Pb + OH^- = (PbOH)_{ads} + e^- \quad [1]$$

$$(PbOH)_{ads} + OH^- = Pb(OH)_2 + e^- \quad [2]$$

$$Pb(OH)_2 + OH^- = Pb(OH)_3 \quad [3]$$

Under most experimental conditions, reaction [3] was found to be the rate-determining step (rds). These results are in general agreement with previous literature for Pb in alkaline solutions (6-11) carried out primarily under galvanostatic conditions.

With the additional use of rotating ring disk electrode methodologies (rrde), it was also previously deduced (5) that as the potential at which PbO was thermodynamically predicted to form was approached [255 mV *vs* RHE (5)], some of the $Pb(OH)_2$ film could dehydrate, forming a small amount of PbO film on the Pb surface, according to reaction [4]

$$Pb(OH)_2 = PbO + H_2O \quad [4]$$

As the potential was extended more positively than about 300 mV *vs.* RHE, cyclic voltammetry revealed the presence of a very large anodic peak (labeled peak A_1), suggested in (5) to be due to the formation of a PbO film at the Pb electrode (reaction [5]), but formed by a different mechanism than that shown in reaction [4]

$$Pb + 2\,OH^- = PbO + H_2O + 2e^- \quad [5]$$

Very little prior literature exists in the area of PbO film formation at Pb electrodes in alkaline solutions. In some of the earliest work (6), it was suggested that a PbO film could be produced along with oxygen by the decomposition of PbO_2, formed at a Pb electrode by the application of low anodic constant current densities (c.d.s.). Later, Glasstone (7) observed the dissolution of Pb under constant current conditions in alkaline solutions at the Pb/

*Electrochemical Society Active Member.
**Electrochemical Society Student Member.

PbO potential, but only PbO_2 was suggested to be the solid reaction product, as seen by the presence of a dark gray film on the surface. A more recent study (8) reported a potential plateau at the expected value for PbO film formation, particularly when low c.d.s. were utilized, although the potential rather rapidly increased towards that for PbO_2 formation. During the constant c.d. reduction of an oxidized Pb electrode, the Pb/PbO potential was observed for relatively long times (8). Upon self-discharge of an oxidized Pb electrode, the colors of Pb_2O_3 and Pb_3O_4 were also observed (8). In the most recent work (9, 10), both constant current and potentiostatic methods were utilized, and PbO was considered to form in two consecutive one-electron transfer steps, although the PbO film product was found to be soluble, leading to $HPbO_2^-$ formation

$$Pb + OH^- \underset{k_{-1}}{\overset{k_1}{\rightleftharpoons}} (PbOH)_{ads} + e^- \quad [6]$$

$$(PbOH)_{ads} + OH^- \underset{k_{-2}}{\overset{k_2}{\rightleftharpoons}} (PbO^-)_{ads} + H_2O \quad [7]$$

$$(PbO^-)_{ads} \underset{k_{-3}}{\overset{k_3}{\rightleftharpoons}} PbO + e^- \quad [8]$$

$$PbO + OH^- \underset{k_{-4}}{\overset{k_4}{\rightleftharpoons}} HPbO_2^- \quad [9]$$

In this paper, the mechanistic aspects of the deposition of a PbO film at a Pb anode in alkaline solutions will be discussed. The experimental methods utilized in this study included CV, potential step methods, and modulated specular reflectance spectroscopy (MSRS). It will be shown that both PbO film deposition and dissolution take place, particularly in the early stages of oxidation. Initially, PbO forms by an instantaneous three-dimensional nucleation mechanism under diffusion control. This hypothesis is consistent with the hysteresis behavior observed by CV, with the shape of the observed potentiostatic i-t transients and also with the results of MSRS. Following this, the PbO nuclei grow to form a thick, porous PbO film at more positive potentials or at longer times. The mechanism of the buildup of very thick PbO films will be discussed in a future publication.

Experimental

The electrochemical experiments were carried out utilizing conventional three-electrode circuitry with a PAR 173 potentiostat coupled to a PAR 175 function generator. In the CV runs, potential sweep rates (s) were typically varied over the range of 5-500 mV/s, and the potential/current curves were plotted on either a HP 7090A or a 7044 X/Y recorder. In the potential step experiments, the current/time (i-t) transients were recorded on a Nicolet 3091 digital oscilloscope, and the data could then be transferred to an IBM Personal Computer.

The experimental arrangement utilized in the MSRS experiments is shown in Fig. 1 (12). In these experiments, 128 repeated identical voltage pulses, each typically 50 msec in length, were applied to a Pb electrode, and the intensity of monochromatic light reflected from the electrode surface was monitored as a function of time by a Photomultiplier Tube (PMT), signal-averaged by a PDP 11-03 computer and then recorded as a function of the time passed after the application of the pulse on an X/Y recorder.

The electrochemical cells utilized in most of this work consisted of two compartments, one for the reference electrode (RE) and one for the working (WE) and counterelectrodes (CE). The WE was constructed with either a Pb disk (99.999% purity; Johnson and Matthey), press-fitted into a Teflon holder, or a Pb disk or chip embedded in epoxy in a Pyrex tube. A Pb disk/Au ring rotating ring disk electrode (RRDE) (Pine Instruments) was also utilized in this work. The details of WE construction, electrode surface preparation, and surface area determination have been given previously (5).

The CE was a high area platinum gauze and the RE was either a reversible hydrogen electrode (RHE) or a saturated calomel electrode (SCE), connected to the main cell by a Luggin capillary. In this paper, all potentials are given with respect to the RHE.

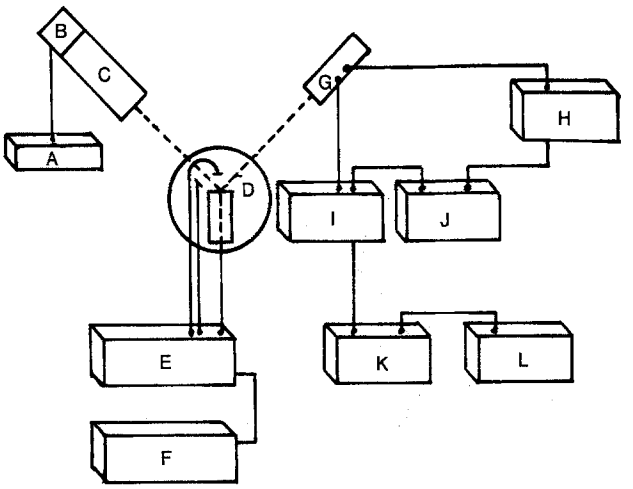

Fig. 1. Block diagram of the MSRS equipment. Lamp power supply (A); lamp (B); monochromator (C); electrochemical cell (D); potentiostat (E); wavefunction generator (F); photomultiplier tube (G); PMT high voltage source (H); current follower (I); integrator (J); computer (K); recorder (L).

All chemicals were of analytical grade and all solutions were made up with thrice distilled water. All experiments were conducted at room temperature and in room atmosphere conditions, as preliminary experiments had shown that the passing of argon through the cell solution did not influence the experimental results.

Results and Discussion

Cyclic voltammetry (CV).—A typical cyclic voltammogram for Pb in a 1*M* NaOH solution is shown in Fig. 2. This CV depicts the steady-state curve observed after several complete cycles of potentials, during which some electrode roughening occurs due to the significant extent of Pb oxidation (and reduction) over this large range of potential.

Three principal anodic features are seen in Fig. 2, the shoulder (A'), peak A_1, and, at higher potentials, peak A_2. Peak A_2 is followed by the occurrence of the oxygen evolution reaction (OER) at a potential greater than about 2V *vs.* RHE. In the cathodic sweep, two peaks are observed,

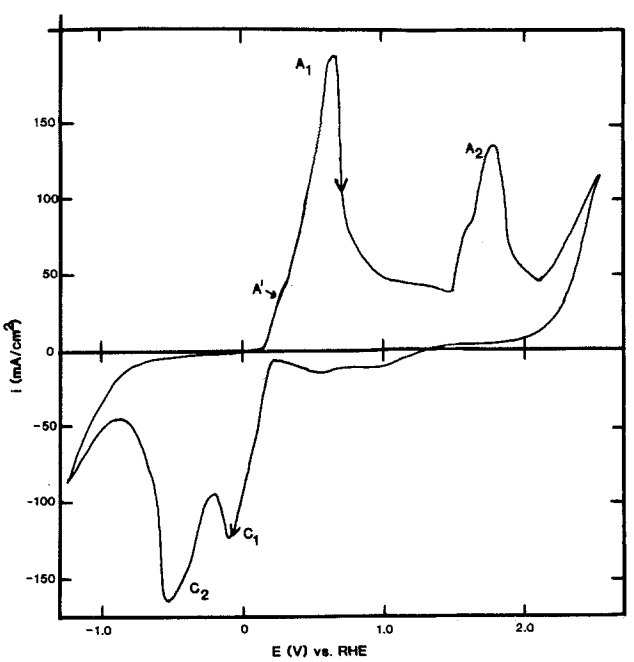

Fig. 2. Cyclic voltammogram obtained with Pb electrode in 1M NaOH solution; s = 50 mV/s; no electrode rotation.

with peak C_1 being associated with the reduction of film material formed in A_1, and C_2 corresponding to A_2. Following peak C_2, hydrogen evolution is observed at the Pb electrode.

It was shown in (5) that the shoulder, A', is associated with $Pb(OH)_2$ film formation and dissolution, thermodynamically predicted to occur at a potential of approximately 115 mV (5), and observed at a potential of approximately 155 mV. This potential is measured as the point where the anodic current departs from the background current, due primarily to double layer charging and reduction of some dissolved Pb species, and hence is not truly a reversible potential. This may explain, in part, the 40 mV difference in the theoretical and observed potentials. Because a significant portion of the $Pb(OH)_2$ film dissolves in the potential range of A' (reaction [3]) (5), a cathodic peak is not observed after reversing the potential scan in the region of shoulder A', as is seen in Fig. 3a.

In the case of peak A_1, the potential obtained by extrapolating the leading edge of peak A_1 to the potential axis is about 220-230 mV in Fig. 3b, which corresponds quite closely to the thermodynamically predicted potential for reaction [5], (255 mV (4)). This close match supports the hypothesis that peak A_1 is related to the formation of a PbO film. It is also important to note that PbO is considered to be the most stable form of the Pb(II) oxides (1), which would be consistent with the prominence of peak A_1 in Fig. 2.

Peak A_2 in Fig. 2 is likely to be related to PbO_2 film formation by reaction [10]

$$Pb(OH)_2 + 2\ OH^- = PbO_2 + 2H_2O + 2e^- \quad [10]$$

The potential at the foot of peak A_2 can only be approximately obtained but is close to 1140 mV, as compared to the theoretical potential for reaction [10] of 1080 mV. A significant overpotential could readily exist here due to the presence of a fairly thick PbO film (about 1 C/cm² up to peak A_2, equivalent to about 5 μm of PbO) at these higher potentials. It is also possible that some of the anodic features observed in Fig. 2, *e.g.*, the shoulder on peak A_2 at about 1.6V may be related to the formation of other Pb oxides, *e.g.*, Pb_3O_4 [red lead, (1)], predicted to form at about 1V *vs.* RHE (4).

A CV of the peak A_1/C_1 region alone is shown in Fig. 4. It is apparent immediately that the anodic and cathodic peaks are of approximately equal magnitude when no electrode rotation is present, indicative of a film deposition and removal reaction without a sigificant contribution of any dissolution processes under these experimental conditions. Also, the linear slope of the leading edges of both peaks is often indicative of reaction rate limitation by the solution resistance. In fact, the inverse of these slopes in Fig. 4 is about 2Ω, which is very similar to the calculated value of the solution resistance of the solution between the tip of the Luggin capillary and the WE.

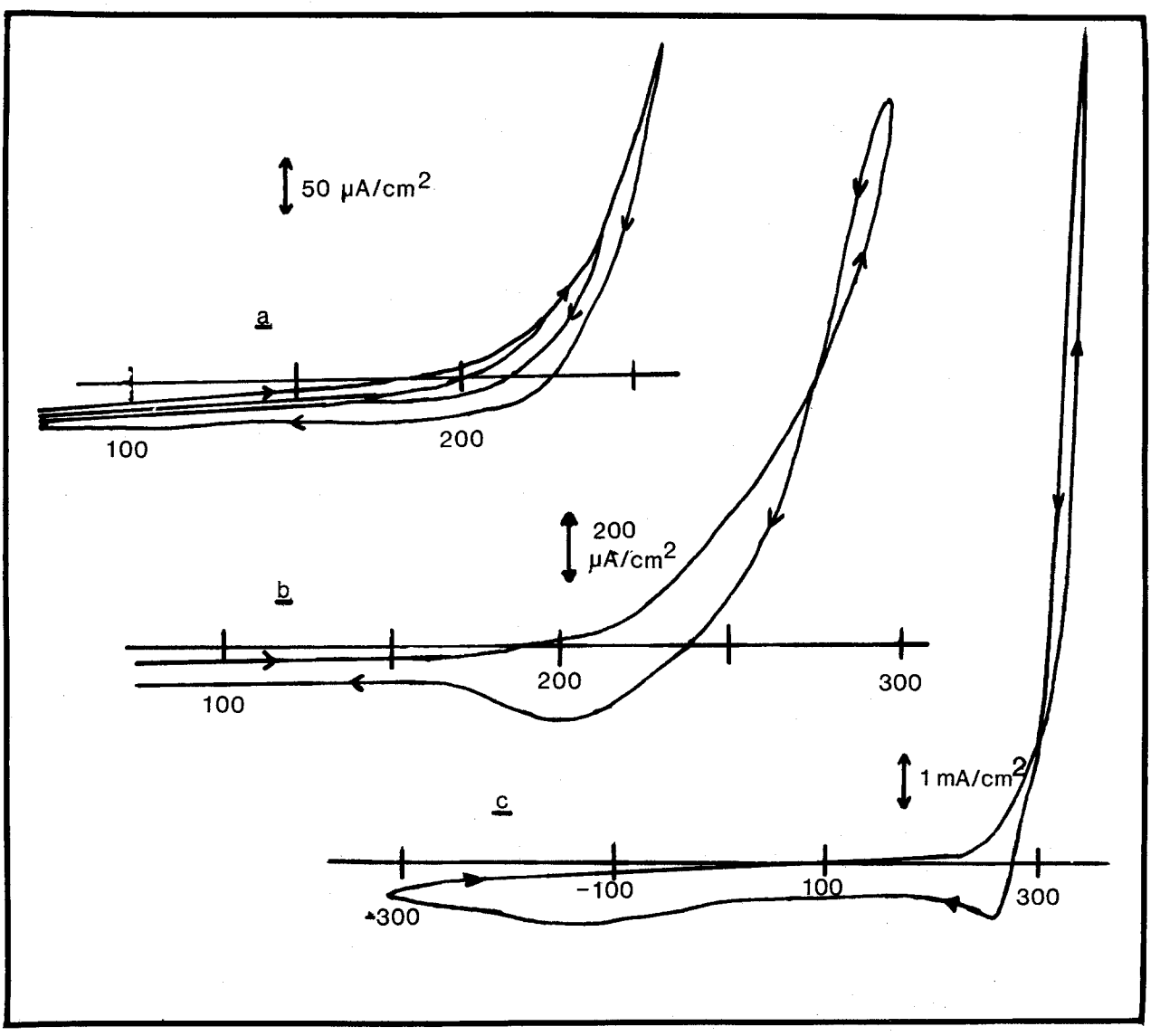

Fig. 3. Cyclic voltammogram at base of peak A_1; s = 50 mV/s; no electrode rotation. Positive voltage limit is 260 (a); 300 (b); 350 mV (c)

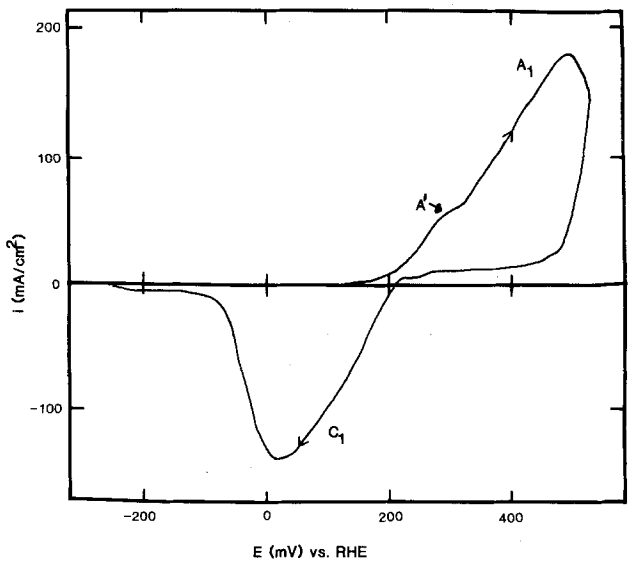

Fig. 4. Cyclic voltammogram obtained with Pb electrode in 1M NaOH solution; enlarged view of peaks A_1 and C_1; s = 50 mV/s.

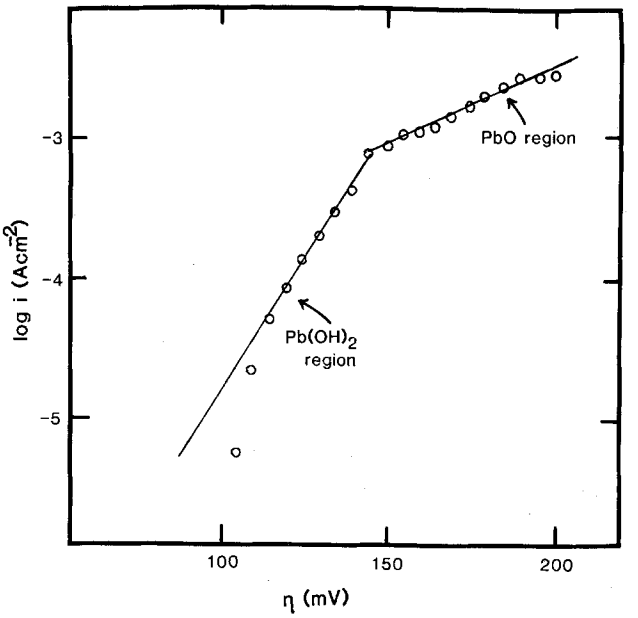

Fig. 5. Tafel plot for Pb in 1M NaOH solution in potential range of $Pb(OH)_2$ and PbO formation. η defined with respect to 155 mV vs. RHE [predicted potential for $Pb(OH)_2$ formation].

Figure 3b shows an expanded view of the CV obtained when the anodic scan is extended to about 290 mV, *i.e.*, in the early stage of peak A_1 (see Fig. 4) and then reversed. A type of "hysteresis" behavior is clearly observed, in which the anodic current is larger in the cathodic sweep than in the anodic scan. This type of behavior has been associated with a nucleation and growth mechanism for film formation (15, 16). This hysteresis has been observed in this work over a wide range of scan rates (5-1000 mV/s), with and without electrode rotation, but only when the positive potential limit was in the range of about 270 to about 370 mV. As 255 mV is the predicted PbO formation potential, this may indicate that PbO film growth initiates by a nucleation and growth mechanism.

It should be noted that the potential could be scanned many times in this potential range (Fig. 3b), without observing any overall increases in the currents due to electrode roughening. Therefore, the hysteresis in Fig. 3b and c cannot be attributed to the development of a higher surface area in the forward sweep, which might then have yielded higher currents in the reverse sweep. Figure 3b also shows, however, that although no significant electrode roughening is occurring in this region of potential, the reverse scan shows only a small cathodic peak. Therefore, it appears that some of the PbO film dissolves in the early stages of its deposition, in accordance with the suggestions in the prior literature (9, 10). Figure 3c shows that when the potential is scanned to about 350 mV or more, a broad cathodic peak appears near −100 mV, and the anodic and cathodic charges match more closely than in Fig. 3a and b. It appears that as more PbO film is formed at higher potentials, proportionately less dissolution occurs. This is consistent with the fairly close match of peaks A_1 and C_1 in Fig. 4.

Potential step experiments.—Steady-state i-E measurements.—The steady-state current/potential data was collected in the range of potential from about 230 to 350 mV *vs.* RHE, *i.e.*, in the range of shoulder A′ and at the base of peak A_1. The potential of the WE was allowed to equilibrate at each potential for about 3 min and then the steady-state current was recorded. The potential was then altered by 5 mV and the process repeated. The measurements were found to be very reproducible, as seen by the similarity of the data when taken in either the anodic or cathodic direction. This again indicates that the Pb electrode surface is not roughening significantly in this range of potential.

Figure 5 shows the Tafel plot of this data, and two distinct Tafel regions can be clearly seen. At lower potentials, the Tafel slope is 27 mV/decade of c.d., which has been shown (5) to be consistent with a $Pb(OH)_2$ film formation and dissolution mechanism (reactions [1], [2] and [3]), with reaction [3] as the rds. The region at more positive potentials has a slope of 70 mV/decade. A second Tafel region has been previously observed, although a slope of 100 mV/decade c.d. was reported (9, 10). In that work, it was proposed that reaction sequence [6], [7], [8], and [9], involving PbO film formation and dissolution, was taking place. A nucleation and growth mechanism for PbO deposition was not invoked.

If reactions [6], [7], [8], and [9] are considered here, with reaction [7] as the rds, then the rate of the overall reaction can be expressed as follows

$$i = z\mathbf{F}\,[k_2[OH^-]\,\theta_{PbOH} - k_{-2}\,\theta_{PbO^-}] \qquad [11]$$

where k_2 and k_{-2} are the forward and reverse rate constants of reaction [7], respectively, and θ_{PbOH} and θ_{PbO} represent the fraction of the Pb surface covered by these adsorbed intermediates.

Assuming that reaction [6] is at equilibrium, θ_{PbOH} can be expressed as follows

$$\theta_{PbOH} = \frac{k_1}{k_{-1}}[OH^-]\exp[z\mathbf{F}\eta/RT] \qquad [12]$$

By substituting Eq. [12] into Eq. [11], the complete current/potential relationship can be expressed as

$$i = \frac{z\mathbf{F}k_2k_1}{k_{-1}}[OH^-]^2\exp[z\mathbf{F}\eta/RT] - z\mathbf{F}k_{-2}\,\theta_{PbO} \qquad [13]$$

At significantly large anodic overpotentials, the rate of the reverse of reaction [7] can be neglected, and hence Eq. [13] can be written as

$$i = \frac{z\mathbf{F}k_2k_1}{k_{-1}}[OH^-]^2\exp[z\mathbf{F}\eta/RT] \qquad [14]$$

From this, the predicted Tafel slope with reaction [7] as the rds is 60 mV/decade of c.d. This is fairly close to the observed 70 mV slope in Fig. 5. It should be noted that if reaction [6] were the rds, the expected Tafel slope would be 120 mV, if reaction [8] were the rds, the slope would be 40 mV, and with reaction [9] as the rds, a slope of 30 mV per decade c.d. would be expected.

If indeed a nucleation and growth mechanism is involved in the early stages of PbO film deposition, as was suggested by the results of the CV experiments (Fig. 3), then the steady-state i-E response should also be controlled by crystal nucleation and growth parameters. However, it will be shown below that the i-t response to a potential step in the region of the second Tafel slope is consistent with the nucleation and growth of PbO, but

under diffusion control. Therefore, it is conceivable that the approach taken above reveals that the nuclei involved in the slow step of the reaction are PbOH or PbO^- species, and that OH^- could be one of the diffusion limited species.

Transient experiments.—In order to test the suggestion that PbO film growth commences by a nucleation mechanism, the current response to a voltage pulse was studied as a function of time. Figure 6 displays a typical current transient (curve a) obtained when a voltage pulse of 290 mV *vs.* RHE, which is in the range of potential in which the hysteresis behavior was observed (Fig. 3), was applied from an initial potential of 0 V. It can be seen in Fig. 6 that the current decays very rapidly in the first 10-20 ms. This initial rapid decay is due to the double layer charging process, expected to be complete in about 50 μs with our experimental setup, but may also involve the deposition of a small quantity of $Pb(OH)_2$ film by a random deposition mechanism (13, 14). It has been previously shown (5) that a current decay of this type could be expected for $Pb(OH)_2$ deposition at potentials less than about 250 mV and, therefore, it is possible that this process is still occurring by the same mechanism at these more positive potentials.

Following the initial decay, a current peak, characteristic of a nucleation process, is observed at about 70 ms. After the peak, the current decreases slowly, although the magnitude of the current both in the peak and postpeak region is clearly highly dependent on solution agitation. Curve b in Fig. 6 shows the i-t behavior when the Pb electrode was rotated at 1560 rpm during the application of the voltage pulse. Clearly a complex combination of reactions involving film deposition and solution transport are occurring. Nevertheless, the evidence of both the current peak in Fig. 6 and the hysteresis in Fig. 3 are highly suggestive of a nucleation and growth mechanism for PbO formation.

In order to test this supposition further, the i-t response from an experiment in which the solution was not agitated by electrode rotation, to minimize the contribution of solution transport controlled currents (Fig. 4, curve b), was modeled on the basis of a particular nucleation mechanism presented in the literature (15). This model involves the three-dimensional nucleation of a film material, *e.g.*, PbO, as hemispherically shaped nuclei initially randomly distributed on the electrode surface, and then growing in all directions, *i.e.*, three-dimensionally into the solution. In contrast, two-dimensional nucleation (16) can be envisioned as involving the formation of thin, tall cylinders of film which grow only laterally on the electrode surface. It should be noted that for either of these cases, two classes of nucleation exist. Instantaneous nucleation involves the initial deposition of a certain number of nuclei, N, which then grow with time, with no other new nuclei forming. In contrast, progressive nucleation involves both a time dependent number of nuclei as well as a time dependent growth rate.

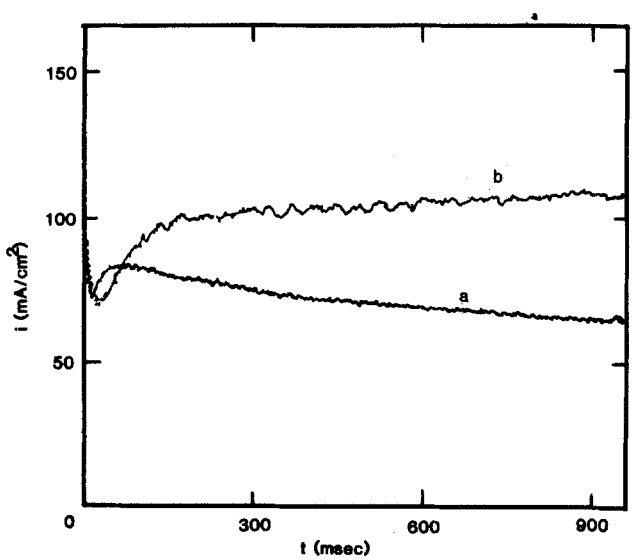

Fig. 6. i-t response to potential step to 290 mV *vs.* RHE. Pb electrode in 1*M* NaOH, no electrode rotation (a); electrode rotation at 26 Hz (b).

Because of the dependence of the current observed in Fig. 6 on solution agitation, as well as the excess of anodic charge to cathodic charge in the CV experiments in the region of the observed "hysteresis," a model of three-dimensional nucleation in which the nuclei grow under diffusion control (15) was chosen for comparison with the experimental results. In the case of PbO nucleation, it is possible that the transport of OH^- species to the growing nuclei could be diffusion controlled, particularly in the region of the current peak observed in Fig. 6. Alternatively, if a sequence of reactions such as [6], [7], [8], and [9] is occurring, then reaction [9] could also be diffusion controlled, in that the rate of PbO formation could be limited by transport of $HPbO_2^-$ away from the electrode surface.

In the case of diffusion controlled growth of PbO nuclei, it is assumed that an expanding diffusion zone exists around each growing nucleus, and that the diffusion zone radius grows in proportion to $t^{1/2}$. As the nuclei continue to grow, their diffusion zones begin to overlap, and therefore the supply of OH^- on the Pb electrode surface and near the nuclei becomes hindered, resulting in diffusion control perpendicularly from the solution to the electrode surface (15).

If an instantaneous nucleation mechanism is assumed, then the relationship between the current, i, at any time, t, is given (15) as

$$i(t) = \frac{n\mathbf{F}D^{1/2}C}{(\pi\, t^{1/2})}[1 - \exp(-N\pi\, kDt)] \qquad [15]$$

where n is the number of electrons passed per molecule of nucleating material, N is the number of nuclei per cm^2 distributed on the electrode surface, D is the diffusion coefficient, C is the concentration of the diffusion limited species, and k is a constant, related to the density and molecular weight of the film material.

If the nucleation mechanism is assumed to be progressive, then the i-t relationship can be expressed as in Eq. [16], where A' is defined as the steady-state nucleation rate constant per site, and N_∞ is equal to the total number of active sites

$$i(t) = \frac{n\mathbf{F}D^{1/2}C}{(\pi t^{1/2})}[1 - \exp(-A'\, N_\infty \pi\, kDt^2/2)] \qquad [16]$$

Equations [15] and [16] contain a number of parameters which cannot be readily evaluated, but the data of Fig. 6 can still be compared with the above models by comparing the i and t maxima predicted by these models with the experimentally observed ones. That is, by taking the first derivative of Eq. [15] and [16] and equating these to zero, the following expressions can be obtained (15):

For instantaneous nucleation

$$t_m = 1.2564/N\pi\, kD \qquad [17]$$

$$i_m = 0.6382n\mathbf{F}DC\,(kN)^{1/2} \qquad [18]$$

and for progressive nucleation

$$t_m = (4.6733/A'\, N_\infty \pi kD)^{1/2} \qquad [19]$$

$$i_m = 0.4615n\mathbf{F}D^{3/4}C(kA'\, N_\infty)^{1/4} \qquad [20]$$

If the square of the current at time, t, is divided by the square of the maximum current, in either the instantaneous or progressive nucleation case, a unitless parameter can be obtained, and therefore, the shape of the entire experimental i-t transient can be compared with the shape predicted for the two possible models considered here (15).

Figure 7 shows a comparison between the experimentally obtained transient, plotted in unitless form (i^2/i_m^2 *vs.* t/t_m), and the theoretically predicted plots for both instantaneous and progressive nucleation under diffusion

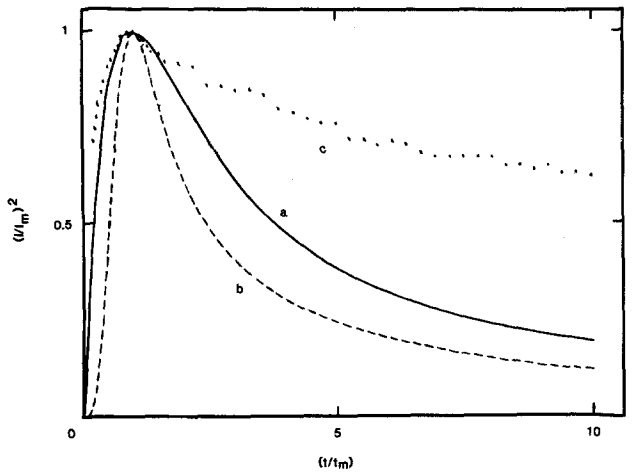

Fig. 7. Comparison of theoretical (curves a and b) and experimental (curve c) curves for three-dimensional nucleation and growth under diffusion control. Instantaneous (a) and progressive (b) models.

control. It can be seen that up to a t/t_m ratio of about 1.5, there is a good fit of the experimental data with the curve for instantaneous nucleation. However, after this time, the experimental curve lies above the theoretical plots for both nucleation mechanisms.

Therefore, these results suggest that PbO film deposition commences by the instantaneous nucleation of a set number of hemispherically shaped PbO nuclei, which then grow three-dimensionally at a rate controlled by the diffusion of OH^- at the edge of the growing nuclei and then from the bulk solution, or, alternatively, of $HPbO_2^-$ away from the electrode surface. This holds at least to times of about 100 ms, after which a deviation from the anticipated i-t behavior occurs. The marked influence of solution agitation on the currents, as seen in Fig. 6 (curve b), emphasizes the likelihood that a Pb dissolution reaction is occurring either in parallel with the nucleation mechanism or in a consecutive step such as in reaction [9]. This would be consistent with the increase in current with electrode rotation, as the product of the dissolution reaction, probably $HPbO_2^-$, is swept into the bulk of the solution away from the electrode surface. It seems much less likely that OH^- could be diffusion controlled in these concentrated solutions.

Modulated specular reflectance spectroscopy study.— The MSRS experiments were carried out in order to gain insight into the early stages of the nucleation and growth of a PbO film in peak A_1. Initial experiments carried out at potentials less than that at which the hysteresis was observed by CV showed no MSRS response, and only if this potential was exceeded were reflectance changes observed.

Figure 8a and b shows several typical MSRS transients which were obtained when the potential was stepped to a potential 10 and 30 mV, respectively, positive of the potential at the onset of the hysteresis observed in cyclic voltammetry (about 260 mV *vs.* RHE). It can be seen in Fig. 8a that the reflectivity of the electrode surface initially decreased. After about 12 ms, the reflectivity began to increase, and when the potential was stepped back to 0 V, the electrode reflectivity increased somewhat before decreasing again. When the larger potential step is utilized (Fig. 8b), the initial decrease in reflectivity is smaller, but then a larger increase in reflectivity is observed at longer times.

These results indicate that the first process taking place is one which decreases the surface reflectivity, e.g., the instantaneous nucleation of a certain number of PbO nuclei, and hence a type of surface roughening on a microscopic scale could be considered to have occurred. These nuclei then grow three-dimensionally, resulting in an increase in reflectivity as the surface coverage of PbO increases. This interpretation implies that the reflectivity of PbO is greater than that of the original Pb surface.

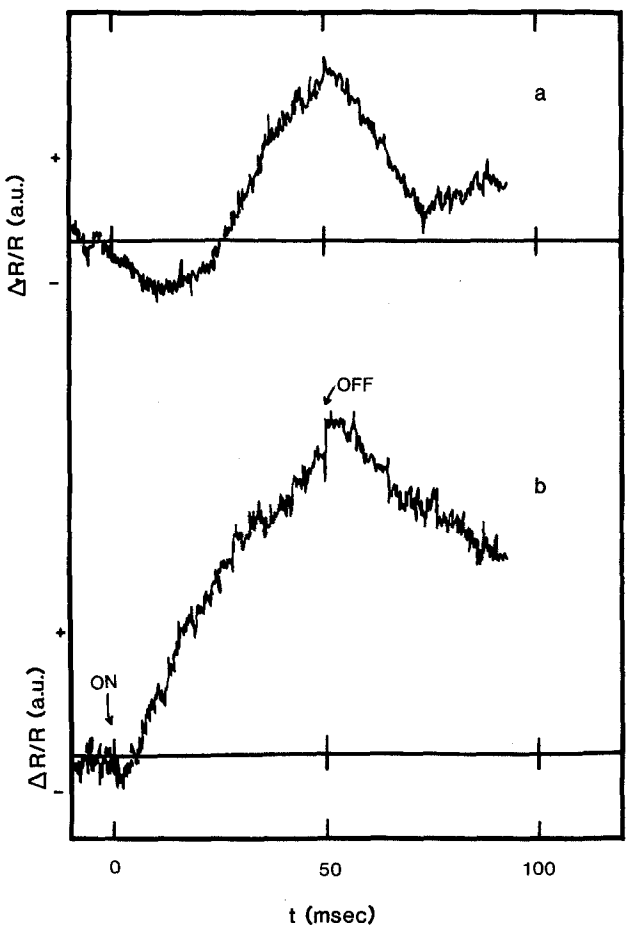

Fig. 8. Surface reflectance as a function of time for Pb electrode in 1*M* NaOH solutions. Pulse length = 50 ms. Potential is stepped to 10 mV (a) and 30 mV (b) positive of the potential at which hysteresis is observed by CV (see Fig. 3b).

At a more positive potential (Fig. 8b), a greater number of nuclei are expected to be present initially, and hence it is anticipated that the Pb surface would become covered by the PbO film more rapidly, yielding a greater increase in reflectivity in a shorter time.

The most important point to note overall is that the reflectivity changes are seen only when the applied potential is in the range of the hysteresis observed by CV. As it seems likely that the initial deposition of numerous small nuclei would lead to a decrease in reflectivity, while the covering of the surface as these nuclei coalesce should lead to an increase in reflectivity, these MSRS results appear to support the hypothesis that a nucleation and growth mechanism for PbO formation applies in the potential range investigated here.

Conclusions

An electrochemical study of the behavior of the Pb anode in concentrated alkaline solutions (1*M* NaOH) has revealed a complex combination of film formation and dissolution reactions. The first stage in Pb oxidation in these solutions has been shown (5) to involve the formation of a $Pb(OH)_2$ film in two consecutive one-electron transfer reactions, followed by film dissolution to form the soluble $Pb(OH)_3^-$ species, with the latter step being the rds.

At somewhat more positive potentials, the PbO formation potential is reached and the deposition of PbO initiates by a three-dimensional instantaneous nucleation process under diffusion control. This mechanism is supported by the reasonably close match, particularly at short times, between the experimental and theoretical (i^2/i_m^2 *vs.* t/t_m) plots, based on such a mechanism. Also, the changes in the reflectivity of the electrode surface with time in response to a potential pulse into the range of PbO formation supports the suggestion of an initial

micro-roughening of the surface (instantaneous deposition of nuclei) followed by a process which increases the surface reflectivity, *e.g.*, coalescence of nuclei in the subsequent growth step.

It is suggested that the diffusion controlled species in the nucleation and growth process may be either OH^- or $HPbO_2^-$, formed as the dissolution product of PbO in this early stage of oxidation. In the latter case, the rate of the nucleation and growth mechanism would be controlled by the rate of removal of $HPbO_2^-$ from the vicinity of the growing nuclei. This would be consistent with the marked effect of electrode rotation (solution agitation) on the i-t transient response as well as the excess of anodic to cathodic charge as observed by cyclic voltammetry.

At longer times or more positive potentials, very thick porous PbO films can be formed, consistent with the outcome of a nucleation and growth film initiation mechanism. A detailed study of the mechanism of formation and the properties of thick PbO films (up to several microns in thickness) will be reported in a future publication.

Acknowledgments

Support of this work by the Natural Science and Engineering Council of Canada is gratefully acknowledged. Thanks are also due to Dr. A. S. Hinman for assistance in the MSRS experiments.

Manuscript submitted June 5, 1986; revised manuscript received Jan. 20, 1987.

REFERENCES

1. "Useful Information about Lead," 1st ed., Lead Industries Association, New York, 1931.
2. W. Hoffman, "Lead and Lead Alloys," 2nd. ed., Springer-Verlag, New York (1970).
3. "Lead-Acid Battery Overview, Materials for Advanced Batteries," D. W. Murphy, J. Broadhead, and B. C. H. Steele, Editors, Plenum Publishing Corp., New York (1981).
4. M. Pourbaix, "Atlas of Electrochemical Equilibria in Aqueous Solutions," 2nd ed., N. A. C. E., Houston, 1974.
5. V. I. Birss and M. T. Shevalier, *This Journal*, **34,** 802 (1987).
6. K. Elbs and J. Forsell, *Z. Elektrochem.*, **8,** 760 (1902).
7. S. Glasstone, *J. Chem. Soc.*, **121,** 2091 (1922).
8. P. Jones, H. R. Thirsk, and W. F. K. Wynne-Jones, *Trans. Faraday Soc.*, **52,** 1003 (1956).
9. S. S. Popova and A. V. Fortunatov, *Soviet Electrochem.*, **2,** 413 (1966).
10. S. S. Popova and A. V. Fortunatov., *ibid.*, **2,** 626 (1966).
11. M. V. Ptitsyn, G. S. Zenin, and K. I. Tikhonov, *ibid.*, **13,** 1144 (1977).
12. A. S. Hinman, Ph.D. Thesis, University of Alberta, 1983.
13. V. I. Birss and G. A. Wright, *Electrochim. Acta*, **27,** 1429 (1982).
14. H. Angerstein-Kozlowska, B. E. Conway, and J. Klinger, *J. Electroanal. Chem., Interfacial Electrochem.*, **87,** 321 (1978).
15. B. Scharifker and G. Hills, *Electrochim. Acta*, **28,** 879 (1983).
16. R. D. Armstrong and A. A. Metcalfe, *J. Electroanal. Chem., Interfacial Electrochem.*, **63,** 19 (1975).

Modeling the Recharge Kinetics of the Positive Electrode Active Mass of a Lead-Acid Battery

Pehr Björnbom

Department of Chemical Technology, Royal Institute of Technology, S-100 44 Stockholm, Sweden

ABSTRACT

A mathematical model has been developed and compared with experimental data from the literature. A characteristic fourfold increase in the Tafel slope with increasing current density found in the experimental polarization curves is predicted by the model. The model is based on the assumption that the positive active mass has a structure with microporous agglomerates forming a macroporous skeleton. During charging, lead ions dissolve from the surface of the lead sulfate crystals, diffuse through the skeleton and into the agglomerates, and finally react on the PbO_2-surface. The fourfold increase of the Tafel slope is attributed to the combined effect of strong pore diffusion resistance in both macro- and micropores. In other respects as well, the model is consistent with published kinetic data.

Pavlov and Bashtavelova (1, 2) recently presented a model for the structure of the positive active mass (PAM) in a lead-acid battery. The PbO_2 crystallites are assumed to build up a microstructure in the form of microporous agglomerates. These agglomerates are linked together to a macroporous macrostructure, or skeleton, which mechanically supports the active material and conducts the electric current.

In hydrophobic oxygen electrodes the catalytic material also forms agglomerates flooded with electrolyte in the cell (3). According to the flooded agglomerate model a characteristic form of polarization curve can be obtained with a doubling of the Tafel slope as current density increases (4). This effect is explained by the fact that the influence of the resistances for pore diffusion of oxygen into the agglomerates becomes greater as current density increases.

Ekdunge and Simonsson (5, 6) have published an accurate investigation of the kinetics of the recharge of PAM including polarization curves. These show a characteristic increase of the Tafel slope with increasing current density. A common hypothesis is that the charge reaction takes place due to the dissolution of lead sulfate succeeded by diffusion of lead ions and reaction on the PbO_2-surface (11, 12). Therefore, the question arises whether this increased Tafel slope can be explained by this hypothesis considering the influence of pore diffusion resistances for the diffusion of lead ions. It is true that the Tafel slope increases three to four times compared to twice for oxygen electrodes, but the PbO_2-structure is more complex than the agglomerates in an oxygen electrode.

Ekdunge and Simonsson tested another hypothesis against their results. This was based on a solid-state reaction mechanism with two consecutive single-electron transfer reactions. The rate equation derived from it fitted well with the experimental points. However, the acid concentration dependence of the ratio between the true exchange current densities for the two reactions strongly deviated from what they derived from their hypothesis. Therefore, they did not accept this hypothesis, although their rate equation can be used as an accurate empirical representation of their rate data.

In the present paper the hypothesis is elaborated that the charge reaction takes place due to the dissolution-diffusion-precipitation mechanism with a strong influence of pore diffusion resistances. Rate expressions are derived on the basis of the structure model of Pavlov and